THE CHANDRA HETGS GRATING X-RAY OBSERVATION OF THE WTTS HDE 245059.

C. Baldovin Saavedra, M. Audard, *ISDC & Observatoire de Genève, Université de Genève, Ch. d'Ecogia 16, 1290 Versoix, Switzerland, (Carla.Baldovin@obs.unige.ch)*, G. Duchêne, *Laboratoire d'Astrophysique de l'Observatoire de Grenoble, 414, Rue de la Piscine, Domaine Universitaire, BP 53, 38041 Grenoble Cedex 09, France*, M. Güdel, *Paul Scherrer Institut, 5232 Villigen PSI, Switzerland*, S. L. Skinner, *CASA, University of Colorado, 389 UCB, Boulder, CO 80309-0389, USA*, F. B. S. Paerels, *Columbia Astrophysics Laboratory, 550 West 120th Street, New York, NY 10027 (USA).*

Weak-lined T Tauri stars (WTTS) are of special interest for the study of magnetic activity in the early stages of a star. Low-mass pre-main sequence stars (PMS) rotate slowly during the early stages of their evolution and spin up as they contract to the main sequence (e.g., Stauffer & Hartmann 1986; Bouvier et al. 1997ab). WTSS are, therefore, at a crucial stage of the early evolution of young stars: magnetic activity and intrinsic X-ray emission are expected to be the strongest during that stage. The lack of significant accretion in WTTS makes them the best-suited objects to magnetic activity in PMS stars, and the impact of stellar flares and X-rays onto their optically thin disks and their planets (e.g., Lammer et al. 2003; 2006; Smith & Scalo 2007).

WTTS show strong X-ray and non-thermal radio emissions (e.g., Feigelson & Montmerle 1999). Compared to ZAMS stars, their X-ray luminosities are very high ($10^{28.5} - 10^{31}$ erg s^{-1}), but they typically show $L_{\rm X}/L_{\rm bol} \approx 10^{-4}$, a dex below the saturation level in late-type stars. WTTS display very high coronal temperatures (e.g., Skinner et al. 1997; Tsuboi et al. 1998), and X-ray flares with temperatures of a few keV are frequently seen (e.g., Tsuboi et al. 1998; Stelzer et al. 2000). Grating observations of PMS stars between the accretion phase and the ZAMS (zero-age main sequence), such as the WTTS HDE 245059, can provide a better understanding of magnetic activity and its evolution in the early stages of stars.

HDE 245059 (HBC 443 = λ Ori X-1; spectral type K1) is an X-ray bright young ($1 - 4$ Myr) WTTS of intermediate mass ($\sim 2\ M_\odot$; Stone & Taam 1985; hereafter ST85). This star rotates fast ($v \sin i \sim 25$ km s^{-1}) and shows no evidence of variability of its radial velocity, suggesting that it is single (Fekel 1997; Alcalá et al. 2000). However, our high spatial resolution near-infrared observations with Keck (obtained by G. Duchêne after the *Chandra* proposal was approved) indicated that HDE 245059 is in fact a close binary (probably two WTTS) with a separation of about 0.88" and position angle of 150 degrees. From the images in the H, K and Brγ filters the magnitude differences between the two components are 1.00 mag in H, 0.91 mag in K and 0.90 in Brγ. These magnitude differences suggest that both components have similar colors.

HDE 245059 is part of the PMS group near λ^1 Ori (O8 III, 13.8$'$ away; $d \sim 400$ pc). The 11 OB stars of the λ Ori star forming region have shredded the parent cloud, and created an ionized region with low obscuration at the center of a ring of molecular clouds (e.g., Maddalena & Morris 1987; Lang et al. 2000). Surveys of the PMS population in the λ Ori region showed that star formation started over the entire region about 8–10 Myr ago and continues in the outer, dense ring of molecular clouds, while it ceased 1–2 Myr ago in the central region (Dolan & Mathieu 1999; 2001; 2002), where the OB stars and our target, HDE 245059, lie. Dolan & Mathieu (2001; 2002) argued that a supernova disrupted the massive cloud core about 1–2 Myr ago, terminating star formation in the central parts of the star forming region. In addition, they found that *all* of the PMS stars near the OB stars are devoid of strong Hα emission, indicating an absence of accretion disks, possibly due to photo-evaporation by the OB stars and perhaps the supernova event. Indeed, HDE 245059 does not show evidence for accretion: its Hα emission is weak with narrow and symmetric profile. Strong Li I λ 6707 Å absorption indicates, however, a young age (Skinner et al. 1991; Alcalá et al. 1996; Padgett 1996; Li & Hu 1998; Alcalá et al. 2000). Furthermore, a 3 σ upper limit in the mm range (<27 mJy at 27.2 GHz = 1100 μm) sets an upper limit of 0.32 $M_\odot$ to the mass of a possible disk (Skinner et al. 1991).

In the X-ray regime, HDE 245059 is among the brightest WTTS: its X-ray luminosity (ST85; Alcalá et al. 2000) is about a percent of its optical luminosity ($\log L_X/L_V = -2.20$; ST85). HDE 245059 also showed some flare activity (Alcalá et al. 1996). ST85 report no photons above 2.5 keV in *Einstein* IPC and a temperature in the range $\log T \sim 6.1 - 6.7$. Archival *ROSAT* and *ASCA* spectra also indicate a surprisingly cool plasma temperature of $6 - 8$ MK for a (double) WTTS. Therefore, we have obtained the *Chandra* High-Energy Transmission Grating Spectrometer (HETGS) X-ray spectrum of HDE 245059 to study its soft spectrum.

The HETGS consists of two sets of gratings, the MEG and HEG, with the ACIS-S CCDs at the focal plane. The MEG covers $2.5 - 31$ Å with a resolution of $\Delta\lambda = 0.023$ Å FWHM, and the HEG covers $1.2 - 15$ Å with a resolution of $\Delta\lambda = 0.012$ Å FWHM.

Observations were performed at three different epochs: $12/30/2005$, $01/07/2006$ and $01/13/2006$ with a total exposure time of 93 ks. The first two observations were done with a roll angle of 308.5deg and the last observation with 294.8deg. Figure 1 shows the ACIS images of the binary for the three different epochs after applying subpixel event position corrections. We detected both components of the binary in X-rays in the zero order images and, despite their close separation, in the grating spectra. The zeroth order light curves indicate that both components showed X-ray variabilty. In particular we observed a flaring event from the weaker southern component during the first epoch observation (Figure 2). We reduced the data from level 1 event file using standard *Chandra* data reduction procedures. We additionally used the subpixel event repositionary algorithm (See Li et al. 2003, 2004) for the zeroth order images only to improve the spatial resolution. For the grating spectra, since the binary is slightly separated, we opted for a zero for the wavelength scale to be in the middle of the binary. In this way the lines from each binary component are on each side of the rest wavelength of the line.

We obtained ± 1 orders for each grating arm, and summed the positive and negative order arms to increase signal-to-noise. The roll angles of the satellite during the observations were such that the MEG dispersion axis was almost completely aligned with the position angle of the binary (almost perfect alignment for the last observation). This orientation allowed us to separate maximally the line spectra of each star in wavelength space.

A preliminary analysis of the spectra indicates that the grating spectra of both components are very similar. They show a combination of cool and hot plasma, confirmed by the presence of several iron lines from Fe XVII to Fe XXV as is shown in Figure 3. The strongest line is Ne X Lyα, at 12.13Å, the Fe lines (in particular Fe XVII at 15 and 17 Å) had mucher lower fluxes, a strong evidence of a high Ne/Fe ratio suggesting an inverse FIP effect. The high continuum due to bremsstrahlung is visible at short wavelengths, and is consistent with hot plasma as detected by the Fe lines of high ionization states (XXI-XXIV). The Ne IX lines, formed typically in a cool plasma, are also well-detected, and show no evidence for high density ($> 10^{12}$ cm^{-3}), since it has a strong forbidden line. The O VII lines are not detected probably due to interstellar absorption.

We performed a preliminary fit of the average grating spectrum in *XSPEC* using a $2-$temperature plasma model with *APEC* (Astrophysical Plasma Emission Code) resulting in best fitting temperatures of 0.6 and 1.6 keV, a total X-ray luminosity of $L_X \sim 9 \cdot 10^{31}$ erg s $^{-1}$ and an upper limit for $N_H < 3.6 \times 10^{19}$. The abundances relative to solar photospheric values (Grevesse & Sauval 1998) are: O$= 0.47$, Ne$= 0.72$, Mg$= 0.20$, Al$= 0.20$, Si$= 0.21$, S$= 0.12$, Ar$= 0.85$, Ca$= 1.03$, Fe$= 0.23$.

Our preliminary analysis clearly detected both components of the HDE 245059 binary. We will continue our analysis of the *Chandra* data of HDE 245059 and determine the spectral properties of the binary.

Acknowledgements

M. Audard, C. Baldovin Saavedra and M.Güdel acknowledge support from Swiss National Science Foundation (SNSF) grants (PP002-110504, 20-58827 and 20-66875.01). Finally, M. Audard received support from *Chandra* award SAO GO5-6012X.

References

Alcalá, J. M., et al. 1996, A&AS, 119, 7
Alcalá, J. M., et al. 2000, A&A, 353, 186
Bouvier, J., et al. 1997a, A&A, 318, 495
Bouvier, J., et al. 1997b, A&A, 326, 1023
Dolan, C. J., & Mathieu, R. D. 1999, AJ, 118, 2409
Dolan, C. J., & Mathieu, R. D. 2001, AJ, 121, 2124
Dolan, C. J., & Mathieu, R. D. 2002, AJ, 123, 387
Feigelson, E. D., & Montmerle, T. 1999, ARAA, 37, 363
Fekel, F. C. 1997, PASP, 109, 514
Kastner, J. H., et al. 2002, ApJ, 567, 434
Lammer, H. et al. 2003, ApJ, 598, 121
Lammer, H. et al. 2006, Space Science Reviews, 122, 189
Lang, W. J. et al. 2000, A&A, 357, 1001
Li, J. Z., & Hu, J. Y. 1998, A&AS, 132, 173
Maddalena, R. J., & Morris, M. 1987, ApJ, 323, 179
Padgett, D. L. 1996, ApJ, 471, 847
Skinner, S. L., Brown, A., & Walter, F. M. 1991, AJ, 102, 1742
Skinner, S. L., et al. 1997, ApJ, 486, 886
Smith, D. S & Scalo, J. 2007, P&SS, 55, 517S
Stauffer, J. R. & Hartmann, L. W. 1986, PASP, 98, 1233
Stelzer, B. 2000, A&A 356, 949S
Stone, R. C., & Taam, R. E. 1985, ApJ, 291, 183
Tsuboi, Y., et al. 1998, ApJ, 503, 894

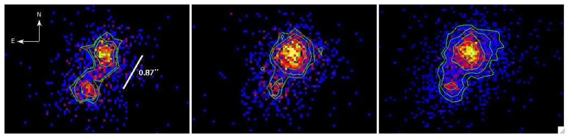

Figure 1: *Chandra ACIS images of the HDE 245059 binary for the three different epochs. Subpixel event position corrections were applied.*

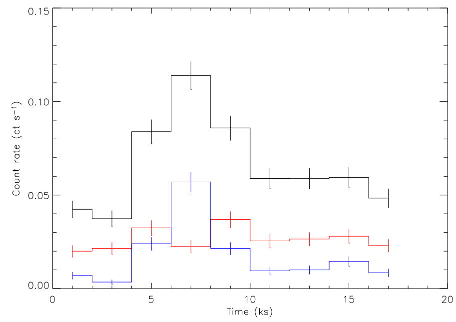

Figure 2: *Zeroth order light curve of the first epoch showing in red the northern component, in blue the southern component and in black the total emission from the binary.*

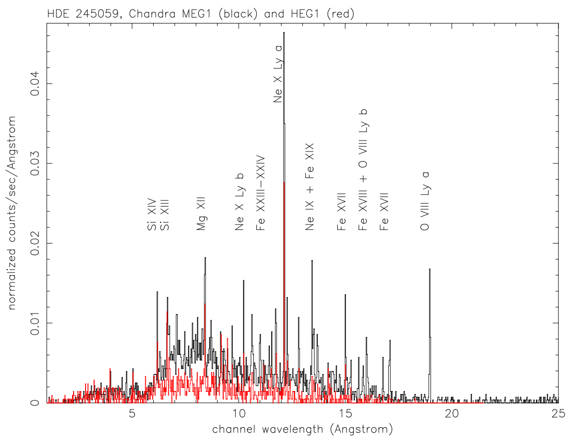

Figure 3: *HETGS average spectrum of the binary HDE 245059 for HEG (red) and MEG (black) grating arms. Bright emission lines are labeled.*